Encapsulation of Peroxide Initiator in a Polyurea Shell: Its Characteristics and Effect on MMA Polymerization Kinetics

Hyeon Jin Kwon[1]
Eun Ju Lee[1]
Mi Rae Kim[1]
Kang Ho Cheon[1]
Hee Jung Park[2]
Kee Yoon Lee*,[1]

[1] Department of Polymer Science and Engineering, Chungnam National University, Daejeon 34134, Korea
[2] Western Seoul Center Korea Basic Science Institute, Seoul 03759, Korea

Abstract: Microcapsule with polyurea shell was prepared from oil-in-water (O/W) emulsion under various agitation speeds (230, 500, and 700 rpm) to encapsulate cumene hydroperoxide (CHP) and *tert*-butyl peroxy-2-ethyl hexanoate (TBPEH). Thus prepared microcapsule size and shell contents were observed to be decreased as the agitation speed increased. Differential scanning calorimetry (DSC) was used to measure and compare the effect on the reaction kinetics of the methyl methacrylate (MMA) radical polymerization in the presence of various initiators. When encapsulated initiator was used instead of unencapsulated initiator the maximum conversion and maximum reaction rate were decreased and the reaction temperature was delayed. The delay in reaction temperature was lager as the agitation speed decreased. In the case of encapsulated CHP at 230, 500, 700 rpm, the temperature at the maximum reaction rate was delayed by 5.8, 3.0, and 0.4 °C, respectively, compared to unencapsulated CHP.
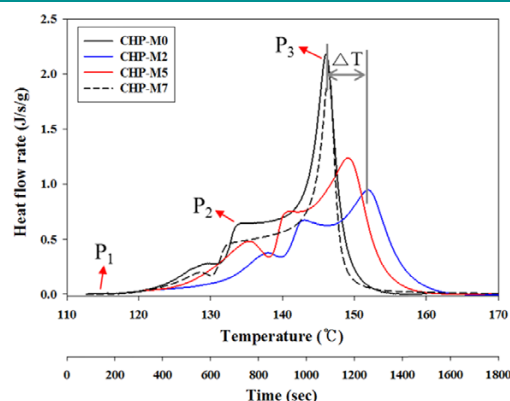
Keywords: microcapsule, encapsulation, polyurea shell, initiator, agitation speed, reaction kinetics, *etc.*

1. Introduction

Microencapsulation is used in various fields such as drug delivery systems, coatings, cosmetics, and self-healings.[1-3] Microcapsule is a small sphere with a uniform wall surrounding the active ingredient. The active ingredient inside is called the core material which ordinarily is functional or reactive. The wall surrounding the core material is called shell or coating material, and mainly lipid and polymer are used for the purpose, interfering with direct contact between the core material and the outside environment.

The first commercialization using microencapsulation technology was a carbonless copy paper developed by Green and Schleicher in the 1950s, and the microcapsules used at that time were made mainly by the complex coacervation of gelatin and gum arabic.[4,5] In the 1960s, Fergason succeeded in microencapsulation of cholesteric liquid crystals using complex coacervation of gelatin and acacia for the use in thermal sensitive display materials.[6] In the 1970s, microencapsulation was utilized for making chemical protection fabrics for soldiers in chemical warfare.[7] Since then this technology has not only been used in the pharmaceutical industry but also in many other products used in everyday life.[8]

There have been many studies to encapsulate various core

materials in order to produce microcapsules suitable for the desired uses. Koochaki *et al.* prepared a microcapsule with a poly(urea-formaldehyde) (PUF) shell by using epoxy as a self-healing coating material as a core material to prevent corrosion.[9] White *et al.* produced PUF shell microcapsules containing dicyclopentadiene inside at various agitation speeds. Thus prepared microcapsule sizes were compared and discussed in connection with agitation speeds. In addition, studies on its storage and release properties have been made on the applicability of microcapsules in corrosion-resistant adhesives as one of the self-healing systems.[10] Möhwald *et al.* encapsulated ibuprofen microcrystals with various types of polyelectrolyte multilayers for use in drug delivery systems and investigated the release of ibuprofen over time.[11] Microcapsules have also been used to improve shelf life in monomer/initiator systems such as in adhesives. Farnood *et al.* prepared microcapsules containing Benzoyl peroxide (BPO) initiator as core material, *i.e.*, double membrane microcapsule was prepared by encapsulating BPO initiator with gelatin-gum arabic inner shell and PUF outer shell to enhance the stability of microcapsules. The shelf life of the microcapsule was also studied in organic solvents.[12] Pojman *et al.* studied the encapsulation of cumene hydroperoxide (CHP) initiator. That is, a microcapsule with a polyurea shell was synthesized, and its shelf life was measured by polymerizing methyl methacrylate (MMA) monomers using frontal polymerization.[13]

In this study, we prepared encapsulated initiator not only to improve its shelf life but also to study the kinetics on radical polymerization. Especially, we studied the change of polymer-

*Corresponding Author: Kee yoon Lee (kylee@cnu.ac.kr)

ization temperature and time delay, maximum conversion rate, and maximum reaction rate according to agitation speed. The result can be used in subsequent process simulations by quantifying the effect of the initiator. For the purposes, each of CHP and *tert*-butyl peroxy-2-ethylhexanoate (TBPEH) was used as the core material. Microcapsule containing an initiator such as CHP and THBEH with polyurea shell was prepared by interfacial polymerization between the oil phase and the water phase at various agitation speeds. Herein, the effect of the agitation speed on the size of microcapsule and the influence of the encapsulated initiator on the radical polymerization were discussed.

2. Experimental

2.1. Materials

Methyl methacrylate (MMA), *n*-heptane, and toluene were available from Samchun Chemical Co. Ltd. (Korea). Poly(vinyl alcohol) (PVA) used as a surfactant and the initiator cumene hydroperoxide (CHP) were from Sigma-Aldrich. Initiator Luperox® 26 {*tert*-butyl peroxy-2-ethyl hexanoate (TBPEH)} was from Seki Arkema Co. Ltd. To prepare microcapsules shell by condensation polymerization, Lupranat® M 20 S {polymeric 4,4'-diphenylmethane diisocyanate (polymeric 4,4'-MDI) containing oligomers of high functionality and isomers} (BASF) and triethylenetetramine (TETA) (Sigma-Aldrich) were used. The structures of the core and shell materials are shown in Table 1.

2.2. Preparation of microcapsules

Microcapsules with polyurea shells were prepared by condensation polymerization of isocyanate and diamine at oil droplet interface in oil-in-water (O/W) emulsion. The oil phase containing both an initiator and polymeric 4,4'-MDI was prepared by adding polymeric 4,4'-MDI (5.4 g) to CHP (43.2 g) (or TBPEH),

followed by stirring for about 5 min. The oil phase was added dropwise to PVA aqueous solution (135.1 g, 1.2 wt%) and the mixture was dispersed at designated agitation speeds (230, 500 and 700 rpm) for about 1 to 2 min. Table 2 shows the sample names prepared according to the agitation speeds. TETA aqueous solution (16.2 g, 22.2 wt%) was added to the emulsion in which the oil phase was dispersed, and the reaction was carried out at 50 °C for 4 h. The microcapsules were obtained by filtration under reduced pressure, followed by washing with distilled water and finally being dried in a vacuum oven at room temperature for 24 h. The dried microcapsules were washed with heptane to remove any remaining organic impurities.

2.3. Microcapsules size distributions and shell thickness

The average particle size of the dried microcapsules was calculated from about 300 particles using an optical microscope (Leica Microsystems, Leica DM500). The particle size distribution was measured as a function of agitation speed when dispersing the oil phase mixture.

The shell thickness of the microcapsules was measured using field emission scanning electron microscopy (FE-SEM) (Carl Zeiss, Sigma HD). Liquid nitrogen-cooled microcapsules were ruptured with a razor blade and sputter coated to platinum coating for 180 s.

2.4. Core and shell contents of microcapsules

Three experiments were conducted to measure core and shell contents of microcapsules. First, the temperature-dependent weight loss was measured using a thermogravimetric analysis (TGA) (Perkin Elmer, Pyris 1 TGA) at a heating rate of 20 °C/min from 30 °C to 600 °C. Secondly, contents of core and shell of microcapsules were measured by ultrasonic pulverization

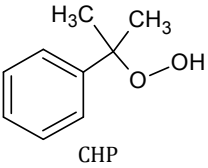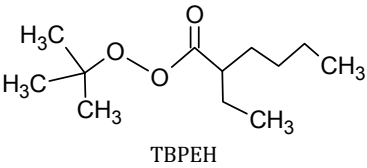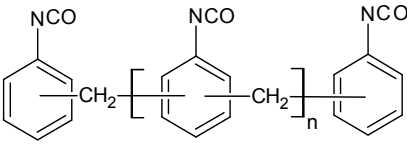**Table 1.** Structures of core (initiators) and shell materials
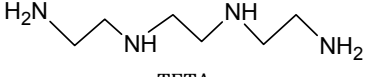
| Core materials (Initiators) | CHP | TBPEH |
| Shell materials | Lupranat® M 20 S | TETA |

Table 2. Microcapsules prepared at various agitation speeds

Agitation speed / Core materials	Cumene hydroperoxide (CHP)	*tert*-butyl peroxy-2-ethylhexanoate (TBPEH)
Unencapsulated	CHP-M0	TB-M0
230 rpm	CHP-M2	TB-M2
500 rpm	CHP-M5	TB-M5
700 rpm	CHP-M7	-

experiment. Approximately 50 mg of microcapsule sample (W_1) was added to 30 mL of toluene and ultrasonicated using a sonicator (Sonics & Materials, VCX 750). The microcapsules were pulverized in toluene for 20 min and cooled for 10 min and this procedures were repeated 3~4 times. The pulverized solution was filtered off under reduced pressure, and dried in an oven at 50 °C for 24 h to measure the weight (W_2) of the microcapsule shell. The core content (%) of the microcapsule was calculated according to the Eq. (1), and the shell content (%) was obtained from 100-(% core content).

$$\text{Core content (\%)} = \frac{(W_1 - W_2)}{W_1} \times 100(\%) \qquad (1)$$

Finally, the contents of core and shell were measured by differential scanning calorimetry (DSC) (Perkin Elmer, DSC 4000). Approximately 3 mg of the microcapsule sample (W_3) was weighed and placed in the pan (W_4). The temperature was raised to 350 °C and then held for 5 min. The weight of the reacted sample with pan (W_5) was obtained and the core content (%) was calculated using Eq. (2).

$$\text{Core content (\%)} = \frac{(W_4 - W_5)}{W_3} \times 100(\%) \qquad (2)$$

2.5. Qualitative analysis of core and shell by Fourier transform infrared (FTIR)

The functional groups of the microcapsule samples before and after pulverization, by following the ultrasonic testing method as was described in section 2.4, were investigated using a FTIR (Thermo, Nicolet iS5 FTIR).

2.6. Reaction kinetics in radical polymerization by DSC

MMA monomer and initiator (or microcapsules) were uniformly mixed, and about 3 mg was placed in an aluminum hermetic pan, and heated at a rate of 2 °C/min from 30 °C to 250 °C to measure the change in heat flow generated during MMA radical polymerization.

3. Results and discussion

3.1. Analysis of chemical structure of microcapsule

Figure 1 shows the FTIR spectra of the microencapsulated CHP and the microcapsule shell obtained from the ultrasonic pulverization experiment.

In Figure 1 the FTIR spectra showed the peaks at 3300, 1648 and 1596, and 690-770 cm^{-1} obviously gave the information that -NH (secondary amine), -C=O (carbonyl), one more and aromatic rings are present, respectively. These peaks were observed in both samples of microcapsules and their shells. In Figure 1(a), peaks attributed to stretching and bending of -CH$_3$ were observed at 2979 and 1445 cm^{-1}, and peaks indicating -C-O- single bond were observed at 1050-1150 cm^{-1}, indicating the presence of CHP in the core. Therefore, we could confirm that microencapsulation was achieved as desired, *i.e.*, CHP was present inside the microcapsule with polyurea shell.
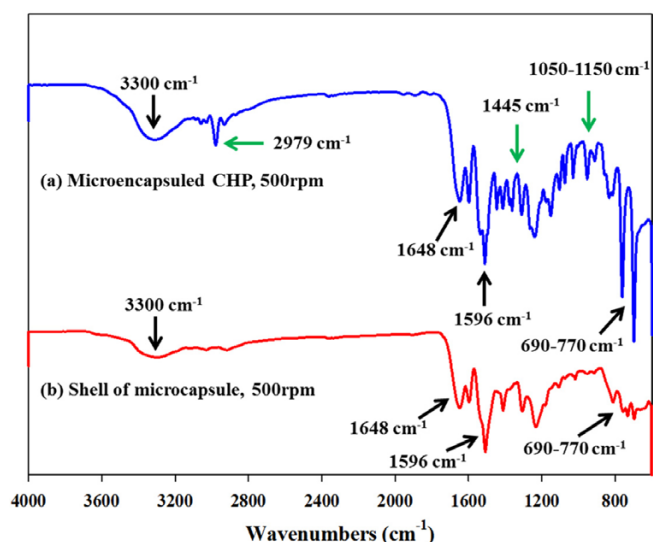

Figure 1. FTIR spectra of (a) microcapsule and (b) microcapsule shell.

3.2. Microcapsule average diameters and size distributions

The dried microcapsules were dispersed in distilled water to confirm the particle size, as shown in Figure 2.

In Figure 2, the sample, CHP-M2 had a relatively larger particle size distribution than CHP-M5 and CHP-M7. The diameters of about 300 dispersed particles were measured in Figure 2(a), (b) and (c), and the particle size distribution is also shown in Figure 2(d). The measured values are represented by three symbols, and the solid line represents a Gaussian distribution curve obtained by regression analysis from the experimental data.

Each average particle diameter of CHP-M2, CHP-M5, and CHP-M7 was calculated to be 272.5, 45.0, and 37.4 μm, respectively. In the case of CHP-M5 and CHP-M7, the particle size distribution was narrower than that of CHP-M2, and their average particle size was sharply decreased as the stirring speed was increased than that of CHP-M2. The particle size tended to decrease with increasing agitation speed in microcapsule manufacturing process. As a matter of fact, increasing the agitation speed provides more force to destroy the droplet than the force to coagulate the oil droplets in the presence of PVA.[14,15]

The microcapsule shell thickness was determined by the FE-SEM to be about 1.4 μm as shown in Figure 3, indicating that a non-porous and dense shell was formed, which could block the release of CHP filled in the microcapsule. In Figure 3, the initiator CHP was observed like a small ball in the shell.

3.3. Determination of core and shell contents of microcapsules

The thermal decomposition behavior of initiator, such as CHP, TBPEH, and various microcapsules were measured using TGA and shown in Figure 4.

As shown in Figure 4(a), the unencapsulated initiator, CHP-M0, started to decompose at about 81 °C and was mostly decomposed at around 188 °C. The microcapsule CHP-M2 started to
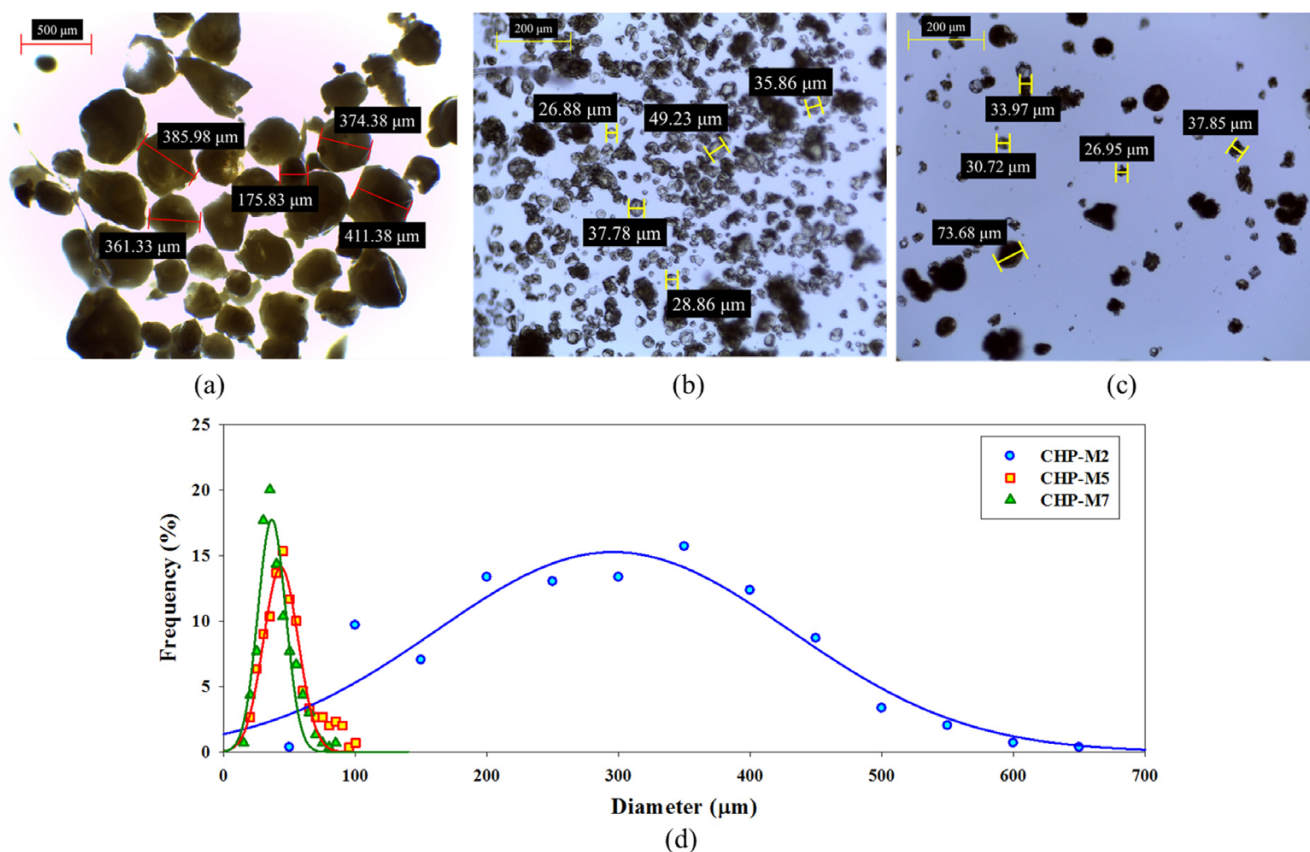
Figure 2. Image of microcapsules dispersed in distilled water (a) CHP-M2; (b) CHP-M5; (c) CHP-M7; (d) microcapsule size distribution.
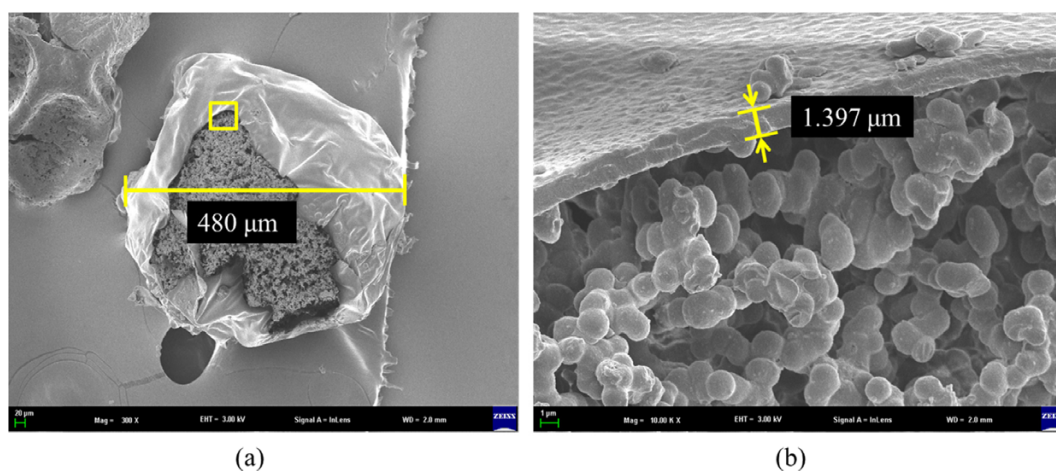

Figure 3. FE-SEM images of CHP-M2 (a) a microcapsule (×300, scale bar: 20 μm) (b) shell of microcapsule (×10,000, scale bar: 1 μm).

decompose at about 124 °C, and decomposed in several steps unlike CHP-M0. When radicals were formed by the decomposition of CHP in the microcapsule, byproducts such as acetophenone, methylstyrene, dicumyl peroxide, and phenol were generally formed.[16] Therefore the slope of the decomposition curve was changed since the byproducts have thermal stabilities different from that of CHP. Actually, the boiling points of acetophenone, methylstyrene, dicumyl peroxide, and phenol is about 208, 116, 130, and 181.7 °C, respectively. The polyurea shell was known to decompose at temperatures above at least 300 °C,[17,18] well in good agreement with our results of about 360 °C as shown in Figure 4 (a). The content (wt%) of the shell was measured to be

40.5, 29.3, and 22.3 wt% in the CHP-M2, CHP-M5, and CHP-M7, respectively, from the remaining weight at the decomposition temperature of the polyurea shell. The thermal decomposition behavior of TBPEH differed from that of CHP in Figure 4(b). That is, TB-M0, TB-M5 and TB-M2 were rapidly degraded at about 94, 98 and 108 °C, respectively. Unlike aromatic CHP, aliphatic TBPEH decomposed without producing any byproducts and its weight was simply reduced. The weight loss of TB-M2 and TB-M5 was about 73.9 and 83.3 wt%, respectively. Therefore, the shell contents were calculated to be about 26.1 and 16.7 wt%.

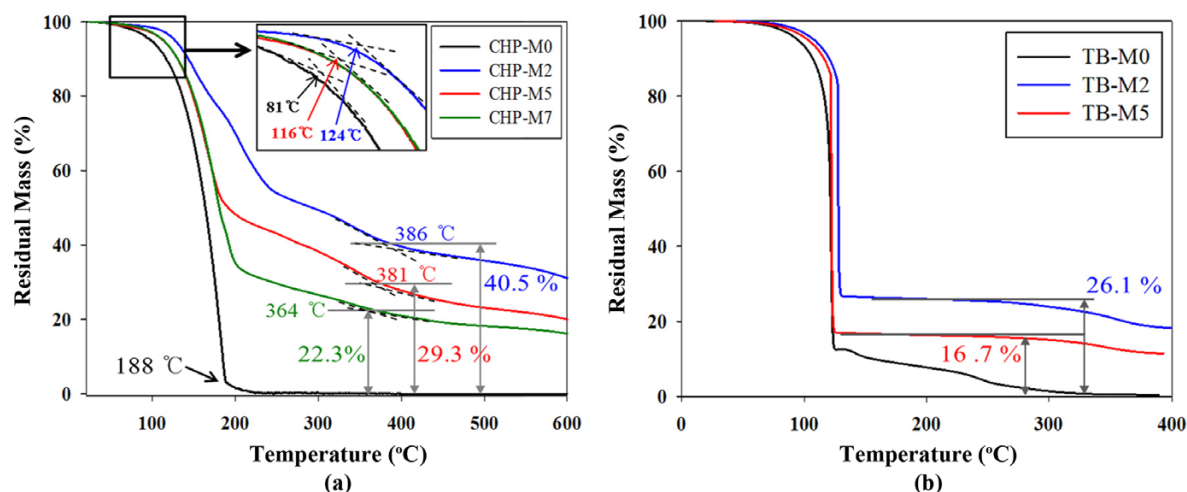In order to determine the core and shell content of the micro-

Figure 4. TGA results of various microcapsules with/without an initiator (a) CHP and (b) TBPEH.

capsule, other methods such as ultrasonic pulverization and DSC experiments were carried out by following the procedure as described in section 2.4 and the results are summarized in Table 3 together with the TGA data.

As can be seen in Table 3, approximately close values of core and shell contents were obtained for three different methods. In the process of dispersing oil droplets in PVA aqueous solution, as the agitation speed increases, the size of oil droplets decreases, and both the number and the surface area of oil droplets increased, so that the shell thickness tended to decrease.[19]

3.4. Effect of encapsulation on reaction kinetics

DSC experiments were conducted to investigate the reaction kinetics of MMA polymerization by using various microcapsules. The change in the amount of heat generated during MMA polymerization was measured, ranging from 30 °C up to 250 °C by rate

of 2 °C/min. The results are shown in Figure 5 and Table 4.

Each point of P_1, P_2, and P_3 shown in Figure 5 shows the onset point at which the polymerization start, rapidly-increasing heat flow rate point, and the maximum heat flow rate point, respectively. In Table 4, ΔT and Δt represents the difference in P_3 temperatures and delayed time between the microencapsulated initiator and the unencapsulated initiator, respectively.

In Figure 5(a), clearly manifested the delay in reaction influenced by the encapsulation, *i.e.*, the temperature at P_3 of CHP-M0 is 146.1 °C, while those of CHP-M2, CHP-M5, and CHP-M7 were 151.9, 149.1, and 146.5 °C, respectively. The relative reaction delay could be numerically compared by the difference in P_3 temperatures and delayed time, that is, ΔT and Δt in Table 4 was 5.8, 3.0, and 0.4 °C and 2.9, 1.5, and 0.2 min for CHP-M2, CHP-M5, and CHP-M7, respectively. Also Figure 5(a) showed the maximum heat flow rate to be 2.18, 2.02, 1.24, and 0.95 J/s/g in CHP-M0, CHP-M7, CHP-M5, and CHP-M2, respectively, indi-

Table 3. Core and shell content (%) depending on agitation speed by TGA, DSC, and ultrasonic pulverization method

| Sample | Agitation speed (rpm) | Thermal degradation | | | | Ultrasonic pulverization | |
| | | TGA | | DSC | | | |
		Core (wt%)	Shell (wt%)	Core (wt%)	Shell (wt%)	Core (wt%)	Shell (wt%)
CHP-M2	230	59.5	40.5	63.2	36.8	59.0	41.0
CHP-M5	500	70.7	29.3	70.6	29.4	69.4	30.6
CHP-M7	700	77.7	22.3	76.2	23.8	75.5	24.5
TB-M2	230	73.9	26.1	73.7	26.3	72.6	27.4
TB-M5	500	83.3	16.7	82.6	17.4	83.0	17.0

Table 4. The P_1, P_2, and P_3 temperatures in the dynamic DSC experiment

Sample	Temperature (°C) at P_1	Temperature (°C) at P_2	Temperature (°C) at P_3	ΔT^a (°C)	Δt^b (min)
CHP-M0	113.0	133.9	146.1	-	-
CHP-M2	122.1	142.0	151.9	5.8	2.9
CHP-M5	120.6	139.6	149.1	3.0	1.5
CHP-M7	114.8	132.5	146.5	0.4	0.2
TB-M0	72.9	104.7	118.2	-	-
TB-M2	85.9	112.4	125.8	7.6	3.8
TB-M5	79.8	108.6	122.5	4.3	2.2

[a]ΔT is the difference of temperatures in P_3 between the unencapsulated and encapsulated initiator. [b]Δt is the difference of delayed time (min) in P_3 between the unencapsulated and encapsulated initiator.
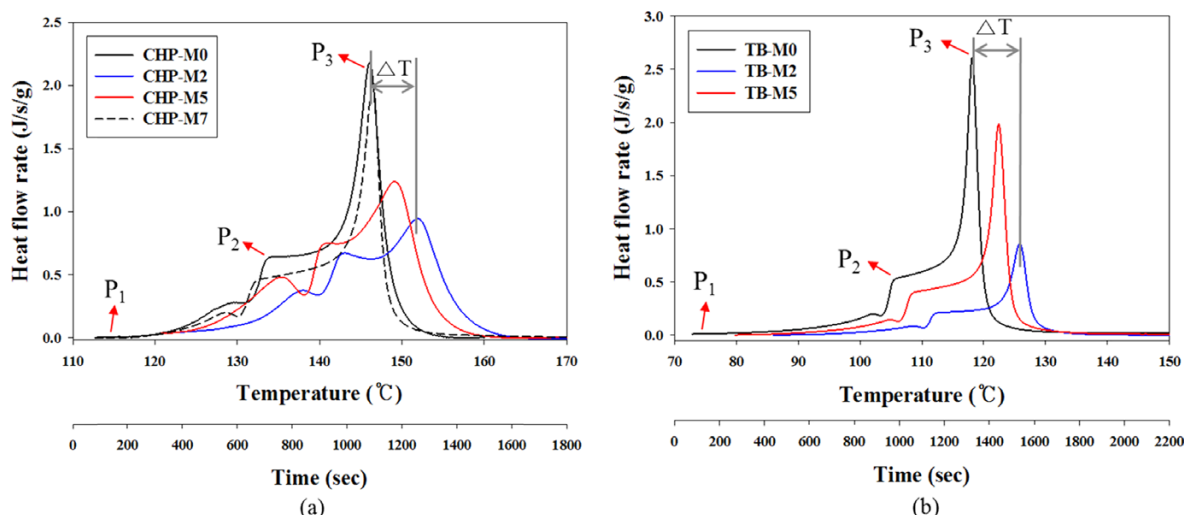
Figure 5. Changes in the heat flow rates in dynamic DSC experiment during MMA polymerization by microcapsule of (a) CHP and (b) TBPEH.

cating again the influence of encapsulation. That is, maximum heat flow rate decreased as the microcapsule size and the shell contents increased. The generated heat flow rate of CHP-M7 showed almost no different behavior around P_3 from that of CHP-M0 due to little effect on temperature delay attributed to small size of microcapsule. In Figure 5(b) using TBPEH initiator, the P_3 temperature was 118.2, 122.5, and 125.8 °C for TB-M0, TB-M5, and TB-M2, respectively, and the maximum generated heat flow rate for TB-M0 was 2.61 J/s/g, while those for TB-M5 and TB-M2 were 1.99 and 0.86 J/s/g, respectively, explaining delayed reaction due to encapsulation.

Figure 5 and Table 4 demonstrated that the initiating reaction was delayed in generated heat flow when an encapsulated initiator was used. Also, it was found that the shell thickness and microcapsule size made temperature and time of the generated heat flow rate temperature and time delayed. The major reason for this effect might be due to the retarded heat transfer to the microcapsule, thereby causing the delay in the release of radical out of the microcapsule. Therefore, it was considered that the time and temperature due to exothermic reaction could be controlled by the agitation speed necessary to disperse oil phase in the process of encapsulating initiators.

In radical polymerization, the conversion increases and the generated heat flows during the expense of monomer at time t after the reaction is initiated by the decomposition of the initiator. The reaction conversion (α) can be expressed as follows shown in Eq. (3), assuming that the generated heat flow rate is proportional to the rate of monomer consumption and the rate of chain growth at time t, as the behavior of heat flow rate is shown in Figure 5.[20]

$$\alpha = \frac{\Delta H|_0^t}{\Delta H_{theroy}} \tag{3}$$

where α is conversion, $\Delta H|_0^t$ is the cumulative enthalpy change at time t and ΔH_{theory} is the total enthalpy change for a theoretically full conversion. The ΔH_{theory} obtained through the dynamic DSC experiment was 510.4 J/g, which value is similar to 543.3 J/g proposed by Roberts.[21]

The cumulative heat flow can be expressed as the conversion shown in Eq. (3) and calculated from the dynamic DSC experiments and are shown in Figure 6. The maximum degree of the conversion of each sample is shown in Table 5.

In Table 5, CHP-M2 showed the lowest maximum degree of conversion (0.785) while CHP-M0 showed the highest value (0.939). In the case of CHP-M5 and CHP-M7, the maximum conversion values were 0.931 and 0.910, respectively. Each maximum degree of conversion of TB-M0, TB-M5, and TB-M2 was 0.975, 0.777, and 0.372, respectively. In Figure 6 and Table 5, it was observed that the maximum conversion decreased as the microcapsule size and the shell contents increased, confirming that the encapsulation process not only delayed the reaction and also decreased the maximum conversion.

The reaction rate ($-r_{MMA}=d\alpha/dt$) could be obtained by time derivative of conversion, which can be expressed with the generated heat flow at time t, as follows shown in Eq. (4). The behavior of reaction rate showed similar tendency as heat flow rate changed in Figure 5.

$$\frac{d\alpha}{dt} = \frac{1}{\Delta H_{theory}} \frac{d(\Delta H|_0^t)}{dt} \tag{4}$$

Table 6 showed the maximum reaction rate to be 3.77×10^{-3}, 3.60×10^{-3}, 2.36×10^{-3}, and 1.74×10^{-3} s^{-1} in CHP-M0, CHP-M7, CHP-M5, and CHP-M2, respectively. In the case of TB-M0, TB-M5 and
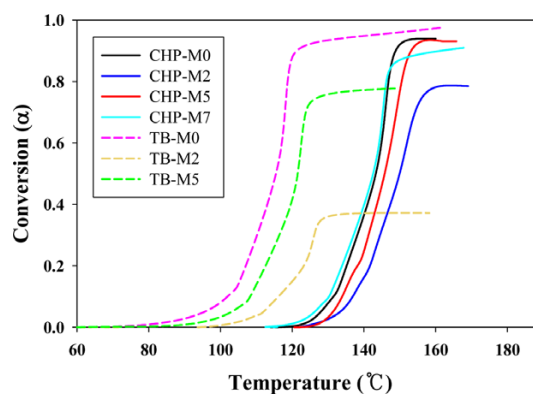

Figure 6. The degree of conversion versus temperature for various microcapsules.

Table 5. Maximum conversion of microcapsules

Sample	Maximum conversion[a]
CHP-M0	0.939
CHP-M2	0.785
CHP-M5	0.931
CHP-M7	0.910
TB-M0	0.975
TB-M2	0.372
TB-M5	0.777

[a]Obtained from dynamic DSC experiment.

Table 6. The P_1, P_2, and P_3 reaction rate in the dynamic DSC experiment

Sample	Reaction rate (s^{-1}) at P_1	Reaction rate (s^{-1}) at P_2	Reaction rate (s^{-1}) at P_3
CHP-M0	1.13×10^{-6}	1.10×10^{-3}	3.77×10^{-3}
CHP-M2	7.47×10^{-7}	1.09×10^{-3}	1.74×10^{-3}
CHP-M5	1.55×10^{-7}	1.12×10^{-3}	2.36×10^{-3}
CHP-M7	3.24×10^{-5}	1.02×10^{-3}	3.60×10^{-3}
TB-M0	1.87×10^{-5}	6.75×10^{-4}	4.80×10^{-3}
TB-M2	3.28×10^{-6}	3.85×10^{-4}	1.58×10^{-3}
TB-M5	1.28×10^{-6}	7.33×10^{-4}	3.65×10^{-3}

TB-M2, the maximum reaction rates were 4.80×10^{-3}, 3.65×10^{-3} and 1.58×10^{-3} s^{-1}, respectively. In MMA radical polymerization using encapsulated initiator, the maximum reaction rate tended to decrease as compared with the case of using unencapsulated initiator. This was similar to the trends in heat flow rate and conversion discussed above.

Therefore, Table 4 and 6 demonstrated that the initiation reaction was delayed due to the encapsulated initiator, and the polymerizing reaction was also delayed. It was concluded that the reaction time and temperature could be controlled by the properties of encapsulation which was determined by operating conditions, such as agitation speed, emulsifier, encapsulating condition, and so on. For example, ΔT and Δt in Table 4 were increased and the maximum reaction rate was further reduced, as the agitation speed decreased in O/W emulsion. The results gave us the information that the use of encapsulated initiator could make the reaction kinetics faster or slower by designing the size and shell contents of microcapsules.

4. Conclusions

In this study, the effect of microencapsulated initiators on reaction kinetics of radical polymerization was investigated. Microcapsules with initiators inside and polyurea shells were prepared by dispersing oil phase in O/W emulsion at various agitation speeds. The composition of core and shell of microcapsules was confirmed by FTIR. The particle size distributions of the microcapsules were measured by the optical microscope and they were discussed by the agitation speeds, *i.e.*, as the agitation speed increased, the size of microcapsule decreased. The shell contents of microcapsules were determined by three methods, TGA, DSC, and ultrasonic pulverization, and they decreased with increasing agitation speeds. The results showed that it is possible to control the microcapsule size and shell contents by adjusting agitation speeds.

Dynamic heating experiments using DSC showed a decrease in heat flow rate, maximum conversion and reaction rate when encapsulated initiators were used in MMA radical polymerization. Also, as the agitation speed decreased, ΔT and Δt in Table 4 which is the difference of reaction temperature and delayed time between the unencapsulated initiator and the encapsulated initiator was increased and the maximum heat flow rate, the maximum conversion, and the maximum reaction rate were further reduced. Therefore, it might be concluded that the use of encapsulated initiator could facilitate the control of the reaction kinetics or delaying reaction time by designing the properties of microcapsules.

Supporting Information: Information is available regarding the experimental data for the determining core contents of microcapsules by DSC measurements. The materials are available *via* the Internet at http://www.springer.com/13233.

References

(1) M. Behzadnasab, M. Esfandeh, S. M. Mirabedini, and M. J. Zohuriaan-Mehr, *Colloids Surf. A: Physicochem. Eng. Asp.*, **457**, 16 (2014).
(2) S. S. Bansode, S. K. Banarjee, D. D. Gaikwad, S. L. Jadhav, and R. M. Thorat, *Int. J. Pharm. Sci. Rev. Res.*, **1**, 38 (2010).
(3) B. J. Blaiszik, M. M. Caruso, D. A. Mcllroy, J. S. Moore, S. R. White, and N. R. Scottos, *Polymer*, **50**, 990 (2009).
(4) B. K. Green and L. Schleicher, NCR Corp, US Patent 2800457 (1957).
(5) B. K. Green, NCR Corp, US Patent 2800458 (1957).
(6) J. L. Fergason, Manchester R & D Partnership, US Patent 4579423 (1986).
(7) D. R. Cowsar, The United States of America as represented by the Secretary of the Army, US Patent 4201822 (1980).
(8) R. Dubey, T. C. Shami, and K. U. B. Rao, *Def. Sci. J.*, **59**, 82 (2009).
(9) F. Safaei, S. N. Khorasani, H. Rahnama, R. E. Neisiany, and M. S. Koochaki, *Prog. Org. Coat.*, **114**, 40 (2018).
(10) E. N. Brown, M. R. Kessler, N. R. Sottos, and S. R. White, *J. Microencapsul.*, **20**, 719 (2003).
(11) X. Qiu, S. Leporatti, E. Donath, and H. Möhwald, *Langmuir*, **17**, 5375 (2001).
(12) M. Raeesi, S. M. Mirabedini, and R. R. Farnood, *Appl. Mater. Interfaces*, **9**, 20818 (2017).
(13) B. McFarland, S. Popwell, and J. A. Pojman, *Macromolecules*, **39**, 55 (2006).
(14) Y. A. Kim, S. H. Kim, J. S. Park, D. S. Lee, J. G. Kim, and J. S. Shin, *J. Adhes. Interface*, **13**, 17 (2012).
(15) M. A. Aravand and M. A. Semsarzadeh, *Macromol. Symp.*, **274**, 141 (2008).
(16) I. D. Somma, R. Andreozzi, M. Canterino, V. Caprio, and R. Sanchirico, *AlchE J.*, **54**, 1579 (2008).
(17) S. Jiang, R. Shi, H. Cheng, C. Zhang, and F. Zhao, *Green Energy Environ.*, **2**, 370 (2017).
(18) W. H. Awad and C. A. Wilkie, *Polymer*, **51**, 2277 (2010).
(19) G. Odian, *Principles of Polymerization*, John Wiley & Sons, Inc., Hoboken, 2004.
(20) E. J. Lee, H. J. Park, S. M. Kim, and K. Y. Lee, *Macromol. Res.*, **26**, 322 (2018).
(21) D. E. Roberts, *J. Res. Natl. Bur. Stand.*, **44**, 221 (1950).